2012

Thermal and Chemical Analysis of Fouling Phenomenon in Condensers for Cooling Tower Applications

Xiaoxiao Wu
xiaoxiao.wu@okstate.edu

Lorenzo Cremaschi

Thermal and Chemical Analysis of Fouling Phenomenon in Condensers for Cooling Tower Applications

Xiaoxiao Wu[1]*, and Lorenzo Cremaschi[1]

[1]Oklahoma State University, School of Mechanical and Aerospace Engineering,
Stillwater, OK, USA
Phone: 405-744-0389, xiaoxiao.wu@okstate.edu, cremasc@okstate.edu
* Corresponding Author

ABSTRACT

Brazed plate heat exchanges (BPHEs) and tube-in-tube heat exchangers (TTHEs) are commonly used in the refrigeration, air conditioning, and food industry as refrigerant-to-water condensers, in which refrigerant rejects heat to water circulating in cooling tower loops. These heat exchangers often suffer from severe fouling issues because as the water in the cooling tower evaporates, the mineral concentration in the remaining water increases. Once the solubility limits are reached, the minerals precipitate and deposit on the heat transfer surfaces: an undesirable yet unavoidable phenomenon. Due to the fouling deposit on the heat transfer surfaces, the thermal resistance between refrigerant and water gradually increases. The fouling resistance depends on several factors such as heat exchanger geometry, heat flux, water quality and water flow rates. The fouling factors penalize the overall effectiveness of the refrigerant condensers and thus must be properly accounted for during the equipment design. Predictions of the fouling allowances during the life service of the condenser characterize the degradation in thermal performance and provide guidelines about the maintenance and service of this type of equipment. In this work, a smooth TTHE was investigated by using a new experimental facility at Oklahoma State University. The aim was to measure the fouling resistance in real time and correlate the data with the water quality and heat flux inside the refrigeration condenser. The fouling resistance in the TTHE was observed to have asymptotic trend and the asymptotic limit was lower than that for BPHEs with soft corrugation angles and higher than that of BHPEs with hard corrugation angles operating at similar conditions. The hydraulic performance was similar as BPHEs with hard corrugation angles. The fouling deposit inside the tube-in-tube heat exchanger was further analyzed by using a CCD camera with a borescope probe and by adopting a chemical digestion process for the fouling particles inside the tubes. Fouling did not deposit uniformly inside the TTHE and it was evident that more fouling was present at the outlet section of the water side. The chemical analysis showed that more than 85% of the fouling material was $CaCO_{3,}$ which was expected from the chemical analysis of the water in critical saturation conditions.

1. INTRODUCTION

In refrigerant to water condensers, heat is rejected from the refrigerant side to the water side, which often circulates in cooling tower loops. Since large amount of inversely-soluble minerals, such as calcium and magnesium contained in the water loop, due to the evaporation process, water became concentrated. When the concentrated water is heated up by the refrigerant inside condensers, the solubility of the minerals decrease and precipitation occurs (Cho *et al.*, 2003). Aside from precipitation, other fouling mechanisms are particulate fouling, biological fouling and corrosion fouling (Haider *et al.*, 1991). Cooling tower water is often pre-treated with biological and corrosion inhibitors, so the last two types of fouling mechanisms might be controlled (Walker, 1976). Minerals concentration, especially calcium concentration was reported to be a main driving force of fouling in heat exchangers. Langelier (1936) proposed an index to evaluate the solubility of $CaCO_3$ in water, which is known as Langelier Saturation Index or LSI. It is mathematically expressed as the algebraic difference between the actual pH of a water sample and its computed saturation pH, which is the pH at which the calcium concentration in given water sample is in equilibrium with the total alkalinity. If the index equals zero, the water sample is in equilibrium state; a plus sign of the index means a tendency of precipitation and a minus sign indicating a tendency of dissolving. This parameter takes into account the total dissolved solids, calcium hardness, total alkalinity, fluid temperature, and the actual pH of the water.

In this work, a smooth TTHE was investigated by using a new experimental facility at Oklahoma State University. The aim was to measure the fouling resistance in real time and correlate the data with the water quality and heat flux inside the refrigeration condenser. Then the fouling resistance for this TTHE was compared with those for BPHEs that had similar heat transfer area and operating with similar water. The heat flux and water mass flow rates were also the same. While these data on the TTHE are preliminary, they serve as starting point for future research on water-side fouling in refrigeration condensers. A second objective of the present work was to provide a verification of the chemical composition of the fouling deposit inside the heat exchanger by using the newly developed test methodology and compare the findings with available data from the literature. A third objective was to investigate the fouling deposit inside the tubes of the condenser. For achieving this goal a special CCD camera with a motorized borescope probe was inserted into the tubes of the condenser and the water side heat transfer surface was visually inspected at various sections of the tube.

2. LITERATURE REVIEW

Several researchers worked on evaluating the parameters that influence fouling. Karabelas *et al.* (1997) conducted experiments by circulating water on one side of the plate heat exchangers (PHE) to control heat flux and water with fouling agents on the other side to promote fouling, observations showed that plates with soft corrugation angle had more tendency to foul than the one with hard corrugation angles. Similar observation was reported by Grandgeorge *et al.* (1998), Cramaschi *et al.* (2011), and Thonon *et al.* (1999). Thonon *et al.* (1999) also investigated in the influence of flow velocity on fouling formation in PHEs experimentally. He claimed that the asymptotic fouling resistance was inversely proportional to the flow velocity. In his experiments, TiO_2, $CaCO_3$ and clay were adopted as fouling agents and the fouling rate was significantly affected by the particle type. For similar particle size and concentration, fouling rates with TiO_2 were much lower than with $CaCO_3$. Experiments regarding to the impacts of internal geometry on fouling formation in tubular heat exchangers was conducted by Li and Webb (2000). In their work, the fouling mechanism was a combination of particulate and precipitation fouling, which was similar as the current work. More minerals deposits were observed in enhanced tubes than smooth tubes, indicating that the asymptotic fouling resistance has a strong dependence on internal geometry of the tubular heat exchangers. In order to identify the similarities and differences of various type of heat exchangers with the same methodology, Bansal *et al.*(2001) tested PHE and double-pipe heat exchangers (DPHE) to study the difference of their thermal and hydraulic performance in fouled conditions. The fouling agent was a mixture of calcium nitrate and sodium sulfate. Research revealed that, for the same flow velocity, the PHE with hard corrugation angle has lower fouling resistance than DPHE. However, the PHE showed higher water side pressure drop than the DPHE. Knudsen and Story (1978) studied the influence of surface temperature on fouling characteristics on a portable test unit. Research showed that more minerals would deposit on the heat transfer surface with higher wall surface temperature; fouling curve increased rapidly within 100 hours and remained reasonably constant after that. Similar observation was reported by Zan *et al*. (2009). The author also reported that fouling formation consists of three periods; an initial period lasted for 3.58 days, followed by a growth period and an asymptotic layer thickness period.

Numerical analysis was also developed to describe fouling characteristic of heat transfer surfaces. Hasson *et al*. (1978) developed a deposition rate model to predict the fouling rate due to $CaCO_3$ deposition on heat exchangers, this model can be applied in various flow and super saturation conditions. Chamra and Webb (1994) proposed a semi-theoretical model in 1994 to predict the asymptotic fouling resistance in enhanced tubes. The model considers parameters like solution concentration, velocity and particle size. Liu *et al*. (1997) proposed a heat mass transfer model to predict fouling, which takes into account the various surface temperature and heat flux. Grandgeorge *et al*. (1998) studied the impacts of flow velocity on fouling formation in corrugated plate heat exchangers experimentally and a fouling rate global model was proposed to predict the asymptotic deposit on the heat transfer surface. Xu *et al*. (2011) investigated the impacts of water quality in a river on fouling formation in plate heat exchangers experimentally and a partial least squares regression (PLS) model was proposed to predict the fouling characteristics.

3. EXPERIMENTAL METHODOLOGY

Water with different fouling potential was developed at our laboratory to replicate the fouling mechanism of refrigerant to water condensers in cooling tower applications. The water fouling potential was evaluated by LSI (Langelier, 1936). LSI was lower than 1 for low fouling potential water and low and slight scaling formation was expected; LSI was between 1 and 2 for medium fouling potential water and moderate scaling formation was expected; LSI was higher than 2 for high fouling potential water, which represent very aggressive water in terms of mineral precipitation. A brief summary of the experimental methodology is given below and more details are given in Cremaschi *et al*. (2011).

From authors previous work, BPHEs with different geometries were tested with different water quality. In order to provide some comparison of the fouling characteristics between BPHEs and tube-in-tube heat exchangers (TTHE), a smooth TTHE with the same heat transfer area as the BPHEs was investigated in this work. A schematic of the test TTHE is shown in Figure 1 and detail specifications are given in Table 1.

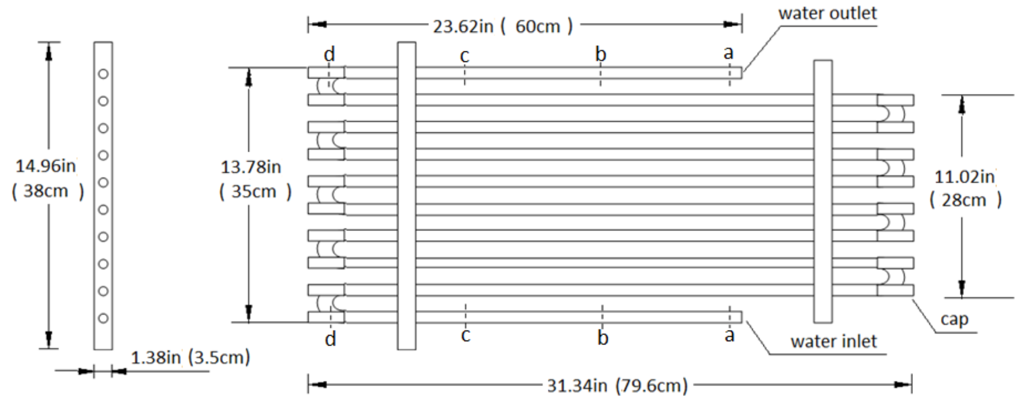

Figure 1: Schematic and dimensions of tube-in-tube heat exchanger[#]

Table 1: TTHE specifications

Dimensions[#], L x W [inch x inch] (cm x cm)	31.34 in x 1.38 in (79.6cm x3.5cm)
Total length and diameter of the tubes (water side)	Total length 297.96in (756.8cm) diameter7/8 in OD(2.22cm)
Number of parallel tubes	10
Heat transfer area [ft^2] (m^2)	4.54ft^2 (0.42 m^2)
Corrugation angle (degree from flow direction)	Smooth tube
Calculated water velocity [ft/s] (m/s)	3.28 ft/s (1m/s)

[#]: These dimensions were taken from a small sample of measurements at OSU laboratory on a commercially available off-the-shelf tube-in-tube refrigerant condenser. They were not given by the manufacturer.

3.1 Experimental apparatus and test conditions

Water was progressively concentrated and controlled in saturated conditions while running through the test TTHE, which was installed in series with a small cooling tower, serving primarily as a mineral concentrator. During operation, water became supersaturated at the tube surface, where water was rapidly heated up by the refrigerant and mineral precipitation occurs due to a drop of solubility. The experimental apparatus mainly consisted of two loops: a water loop and a refrigerant loop, sharing the same test TTHE. In the water loop, about 25% of the total flow rate through the test TTHE was diverted to the small cooling tower, in order to evaporate water at ambient temperature and to control the solubility of the minerals in the water close to saturation conditions. Table 2 provides the list of independent variables that were set and accurately controlled during the fouling test; the test conditions were also in agreement with the recommendations in the AHRI 450 guidelines (AHRI, 2007).

Table 2: Test conditions for the fouling tests on TTHE condensers

Independent variables controlled during the fouling experiments	Nominal value and tolerances during the fouling experiments
Water side	
Entering water temperature (T_{EWT})	85.03 ± 0.05°F (29.4±0.03 °C)
Water flow rate ($\dot{V}_w$)	4.65 gpm[#] ± 0.03 gpm (29.3 × 10^{-5} m^3/s)
Cooling tower water LSI	2.1 – 3.5 (with modified pH @ 9.3-9.6)[+]
Refrigerant side	
Saturation condensing temperature ($T_{sat,r}$)	105.5 °F ± 0.5°F (41 and ± 0.3 °C)
Degree of superheat (ΔT_{SH}).	65.0± 0.5°F (36.1± 0.3 °C)
Refrigerant mass flow rate ($\dot{m}_r$)	3.50± 0.02 lb_m/min (26 × 10^{-3} ± 15 × 10^{-5}kg/s)

[#]: Set at 3 gpm/ton of cooling capacity. Estimated TTHE capacity was about 1.5 tons of refrigeration (5.3 kW or 18,000 Btu/hr)

[+]: LSI representative of strong to severe scale formation conditions

3.2 Data reduction and uncertainty analysis

The fouling test was conducted until the measured fouling resistance was at least 85% of the asymptotic fouling resistance or until waterside pressure losses exceeded the maximum pumping head available in the water loop. The data reduction of the measurements for fouling resistance in TTHE was carried out according to the steps summarized in Cremaschi *et al*. (2011). The logarithmic mean temperature difference, LMTD, was based on the refrigerant saturation temperature in agreement with the AHRI 450. This LMTD approach does not consider either the degree of superheat or sub-cooling on the refrigerant side. In the current work, the degree of superheat was controlled to 65°F (36.1°C) in order to replicate operating conditions similar to the ones of actual condensers in cooling tower applications and the degree of sub-cooling was about 13°F (7.2°C).

A complete and thorough uncertainty analysis was conducted according to the uncertainty propagation method suggested by Taylor & Kuyatt (1994). Details on the error propagation analysis for the fouling measurements can be found in authors previous work (Cremaschi, *et al*., 2011). The overall uncertainty on the fouling resistance was about 65% for fouling resistance lower than 1.0×10^{-4} ft^2-°F-hr/Btu (1.8×10^{-5} m^2-°C/w) and 36% for fouling resistance between 1.0×10^{-4} to 1.0×10^{-3} ft^2-°F-hr/Btu (1.8×10^{-5} to 1.8×10^{-4} m^2-°C/w). The outcomes from the uncertainty analysis were included in the data reduction in the current work and are integrated in the experimental results and discussion part. The results from the tests on TTHE provide a comparison between the fouling allowance measured in the present work and the data available in previous work (Cremaschi *et al*., 2012). They also serve as a starting point for future research on waterside fouling phenomena in smooth and enhanced tubes condensers.

4. RESULTS AND DISCUSSION

4.1 Fouling deposit chemical analysis

After two months of testing, the condenser was opened from the caps located at the end of each tube and a layer of light yellowish fouling deposit on the caps surface was visually observed, as shown in Figure 2(a). These images were taken by a conventional digital camera. It is evident that mineral precipitation occurred and the heat exchanger experienced fouling. The fouling deposit material was sampled, as shown in Figure 2(b), and composition analysis was conducted by chemical digestion at Soil, Water and Forage Analytical Laboratory (SWFAL) at Oklahoma State University. Chemical analysis showed that more than 85% of the fouling deposit was $CaCO_3$; the amount of Mg was less than 0.5%; the amount of Fe, Cu, Zn were within 5%. During the fouling test, fouling deposited on every component throughout the entire water loop, including water tank, electric heater, cooling tower, water pumps, heat exchangers, and water pipes. In particular, the amount of fouling on the test TTHE was about 4 to 5% of the total amount in the water loop. When considering the area of the entire test set up without the TTHE, it was estimated that the mineral precipitation mass flux was about 4.4×10^{-5} lb/in^2 (3 mg/cm^2) and the precipitation mass flux in the TTHE was about 3.7×10^{-5} lb/in^2 (2.6 mg/cm^2). Considering the measurement uncertainty in the fouling deposit mass sampled from the TTHE and the approximation for the effective area exposed to fouling in the batch tank and in the cooling tower tank, the two precipitation mass flux were similar. In the TTHE the water had the highest bulk temperature but in the water tank, water reached the highest local temperature near the heating elements. In the cooling tower, aeration is also promoted and the production of $CaCO_3$ is locally increased according to the reaction given in Equation (1):

$$Ca(OH)_2 + CO_2 \rightarrow CaCO_3 + H_2O \tag{1}$$

These observations support the fact that the mineral precipitation mass flux was practically the same for the entire system and the analysis provide an order of magnitude of the mineral precipiation mass flux for the case of high water fouling potential.

(a) condenser caps with fouling deposit on them (b) fouling deposit material sampled

Figure 2: Fouling samples from TTHE condenser

In the process of sampling fouling deposit material from the tube caps, an observation was made that, the thickness of fouling varies according to the location of the cap. Thicker deposition appeared at the water outlet, where the water temperature was almost 10°F (5.56°C) higher than the water inlet. This phenomenon can be explained by the solubility of minerals in water since the solubility of $CaCO_3$ decrease with increasing temperature as shown in Figure 3. More minerals tend to precipitate at higher temperature resulting in a larger amount of fouling deposit at the outlet of water tube than the inlet. In order to verify this assumption, a CCD camera with an extended bore-scope probe was used to take digital images inside the smooth tube-in-tube heat exchanger, as shown in Figure 4. The CCD camera had a high resolution short focus charge-coupled device camera and included a motorized 1 meter extended mini probe head, which was inserted in the condenser tubes.

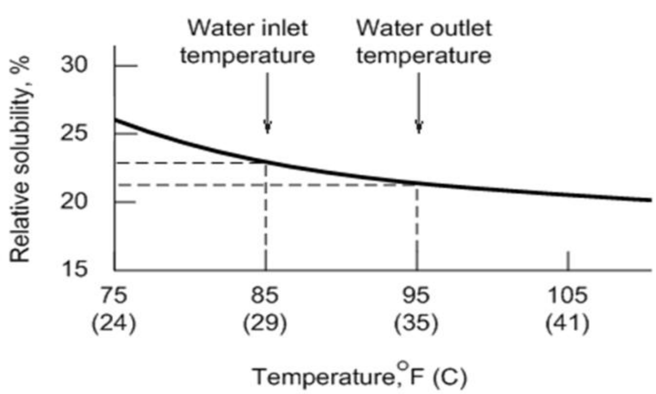

Figure 3: Solubility of $CaCO_3$ with temperature change (adapted from (Flynn & Nalco, 2009))

The bore-scope of the CCD camera was inserted inside the water inlet and outlet tubes of the TTHE and digital images were taken at various locations indicated as “a”, “b”, “c”, and “d” in Figure 1. The corresponding images of the fouling deposit layers are shown in Figure 4; the top images are for the tube at the water inlet section while the bottom images are for the water outlet section. The four images are labeled (a), (b), (c) and (d) and they represent the fouling conditions at the entrance, in the first half, in the second half and at the end of each tube. In order to make a comparison of fouling appearance, the photos were taken at the same axial location inside the inlet and outlet tubes. Thicker layer of fouling was visually observed inside the outlet tube than the inlet tube and photo (d) in Figure 4 supports this observation.

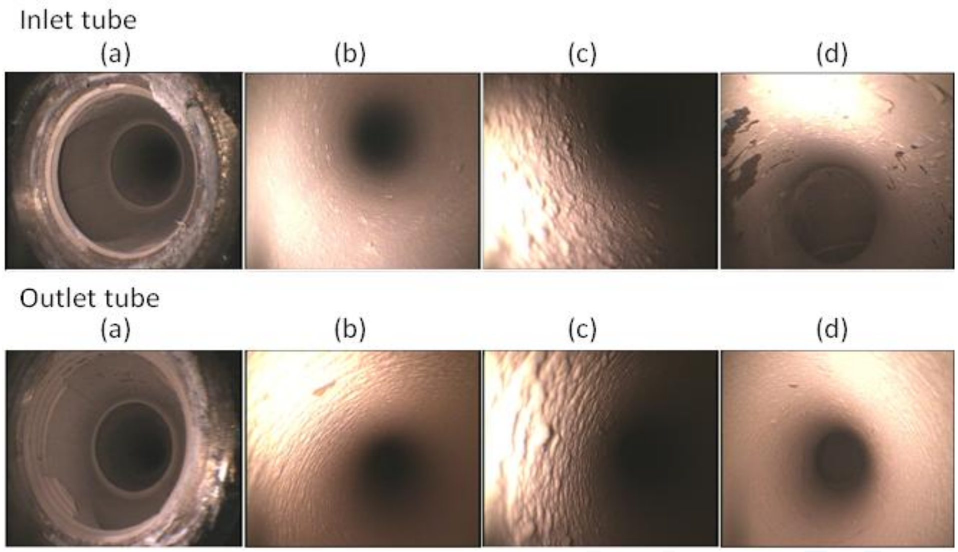

Figure 4: Images of fouling deposit inside smooth tubes of a tube-in-tube heat refrigerant condenser

Attempts were also made to take fouling pictures inside the BPHEs, as shown in Figure 5. The authors cut the plate heat exchanger with a bench saw. It was observed that the thin metal plates plastically deformed due to the heat generated during the cutting process and the surfaces were contaminated by the cooling fluid of the saw. Inevitably some of the fouling deposit material was destroyed and removed. However, some fouling deposit was still visible inside the mini channels as shown in the circled region in Figure 5.

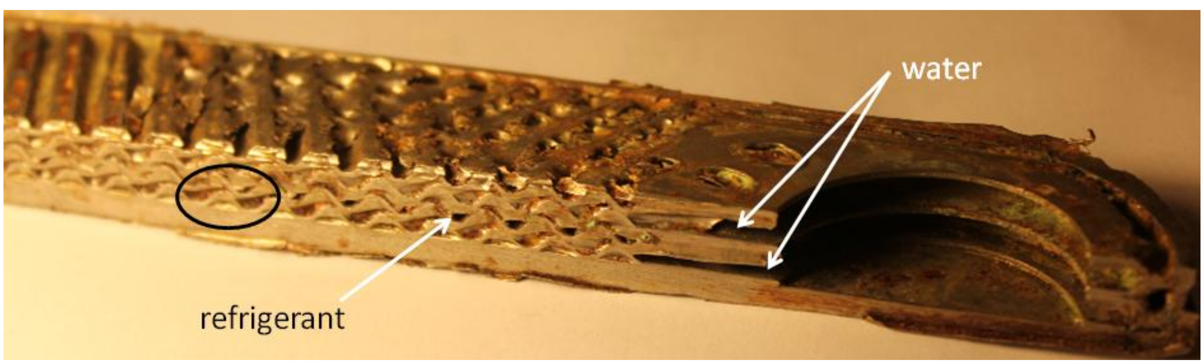

Figure 5: Images of fouling deposit inside a BPHE

4.2 Fouling heat transfer analysis

Figure 6 shows a comparison of measured fouling resistance between TTHE in the current work and BPHEs of authors previous work with same test condition and same quality of water. A1 indicates BPHE with soft corrugation angles of 30°, and A2 indicates BPHE with hard corrugation angle of 63°. The TTHE tested in the current work had the same nominal heat transfer area as A1 and A2 plates. Detail information of BPHEs geometry and experiments on A1 and A2 plate was given in Cremaschi *et al.* (2011, 2012)

In Figure 6, the A1 plate achieved a fouling resistance of about 1.0×10^{-3} ft^2-°F-hr/Btu (1.8×10^{-4} m^2-°C/w) in 30 days, as shown in diamond points. A2 plate reached a fouling resistance of 1.3×10^{-4} ft^2-°F-hr/Btu (2.4×10^{-5} m^2-

°C/w) in 55 days, shown as square points. A1 and A2 plates had identical geometry; the only difference was that A1 had a soft corrugation angle while A2 had a hard angle. The experimental results clearly showed that the fouling resistance for A1 plate was almost one order of magnitude higher than A2 plate. Water in between the plates flows from the inlet to the outlet mainly in the mini-channels created by the corrugations on the plates, which are stacked on each other and rotated by 180°. Water also crosses the ridges from one mini-channel to the adjacent one, thus moving in a zig-zag pattern. The extension of the angle of the zig-zag pattern depends on the chevron angle and depth of the corrugations. Different local velocities and local turbulence intensity in between the plates are expected between the A1 plate and the A2 plate. The authors speculate that higher local velocity and higher degree of zig-zag were the A2 plate with respect to the A1 plate. Thus higher convective heat transfer coefficients and higher water side pressure drop in between the plates in A2 plate could be expected. This high level of local velocity and turbulence seems to promote the removal mechanism of the fouling deposit, resulting in a lower overall fouling resistance. Stasiek *et al*. (1996) investigated the influence of corrugation angles on flow and heat transfer phenomenon in plate heat exchangers. Their research revealed that the increase of corrugation angle would promote local Nusselt number, which is proportional to $Re^{2/3}$, which supported our speculation that higher local turbulence occurred in the A2 plate with hard corrugation angles. For the smooth tube-in-tube heat exchanger with same heat transfer area and operating conditions, its measured fouling resistance data was shown as cross points in Figure 6. Since the TTHE had larger water flow cross-section area than the BPHEs, the local velocity was expected to be fairly low. The measured fouling resistance was in between A1 and A2 plate; after 60 days of operation, a fouling resistance of 4.8×10^{-4} ft^2-°F-hr/Btu (8.6×10^{-5} m^2-°C/w) was obtained. The effects of geometry and local velocity were combined in this test, leading to a fouling behavior in between the A1 and A2 plate; similar phenomenon was reported by Bansal *et al*. (2001). However, more tests at different velocities and various tube diameters would be necessary for further investigation of the fouling behavior on tube and tube type condensers.

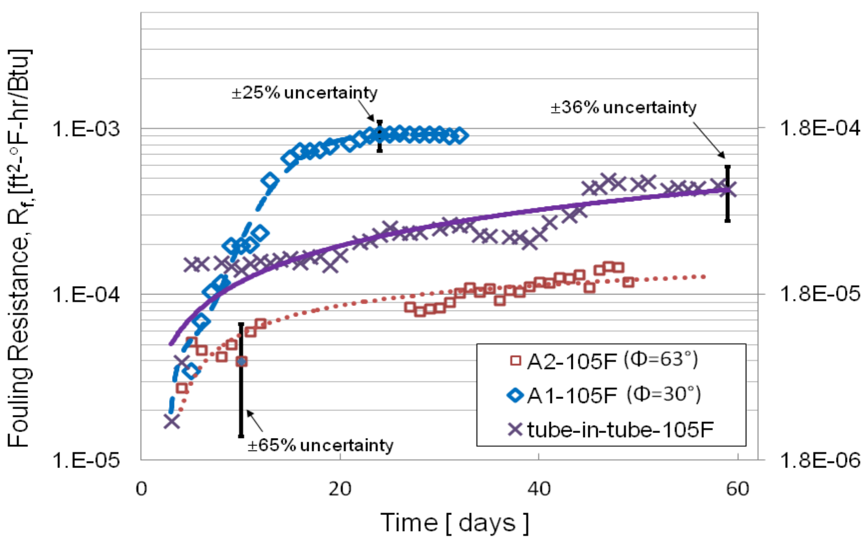

Figure 6: Comparison of measured fouling factor between TTHE (tube-in-tube) and BPHEs (A1&A2)

Figure 7 shows the water temperature difference between inlet and outlet of the test condenser. Three heat exchangers, A1, A2 and TTHE were compared. All of them were tested with same operating conditions. Since entering water temperature and the water flow rate were controlled to be constant for all the tests, the decrease of leaving water temperature has similar trend of the heat flux. A1 plate, shown as diamond points, had a sharp temperature drop of 1°F (0.56 °C). The heat fluxes in clean conditions were about 3,424 Btu/hr- ft^2/ (~11 KW/ m^2), and after 30 days of fouling test, the heat fluxes decreased by 28%. The A2 plate, with a hard corrugation angle of 63°, experienced a small decrease in the heat flux across the plate; the heat flux degradation was within 5% in 55 days with respect to heat flux in clean conditions. The trend of heat transfer degradation in TTHE was quite similar to the A2 plate. During 60 days of operation, a decrease of 8% in heat flux was observed, the water temperature difference across the test condenser for A2 plate and the TTHE had similar slope during first 40 days of operation. By the end of the fouling test, the temperature difference for the TTHE decreased by as much as 0.7°F (~0.4°C).

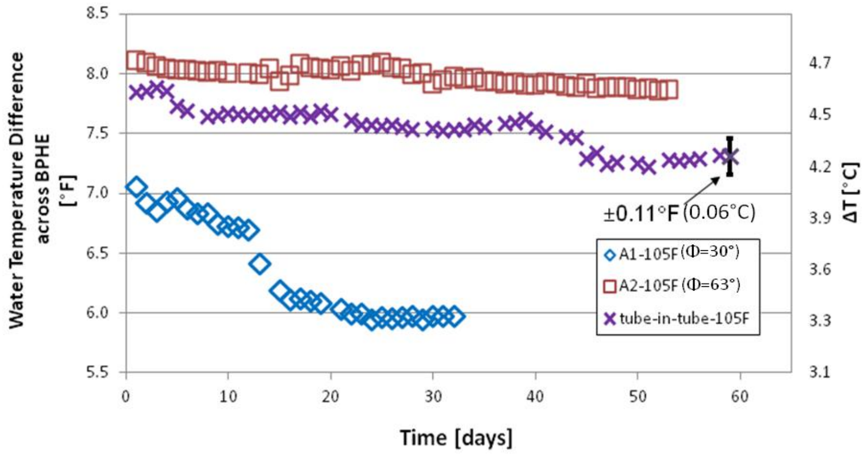

Figure 7: Comparison of measured water temperature difference between TTHE (tube-in-tube) and BPHEs (A1&A2)

The hydraulic performance of the test heat exchangers is presented in the form of pressure drop penalty factors (PDPF) in Figure 8. Pressure drop across the test condenser in clean conditions are also given in the legend. PDPF values for each test were calculated according to Equation (2) and they represented the ratio of water side pressure drops measured in fouled conditions and the corresponding ones measured in clean conditions. For instance, the A2 plate had a PDPF of 1.1 after 55 days of fouling tests, which means a 10% of increase of pressure drop in fouled conditions was observed by the end of the test with respect to clean conditions. A1 plate experienced a localized blockage of the mini-channels and as a result, the pressure drop increased by 30%.

$$\text{PDPF} = \Delta p_{w,f}/\Delta p_{w,c} \tag{2}$$

The cross points in Figure 8 indicate the pressure drop across the TTHE tested in the current work. Since the TTHE had larger free flow cross sectional area than the plate-type heat exchangers, it was not subjected to severe clogging due to fouling. As shown in Figure 8, at about day 5, the tube PDPF increased suddenly. This phenomenon is generally due to localized flow blockage from particulate fouling, in which particles attached on the surface and created a significant resistance to the water stream. After day 5, the increase of the PDPF for the TTHE was minor and the pressure losses were about 10% higher than the initial pressure drop in clean conditions.

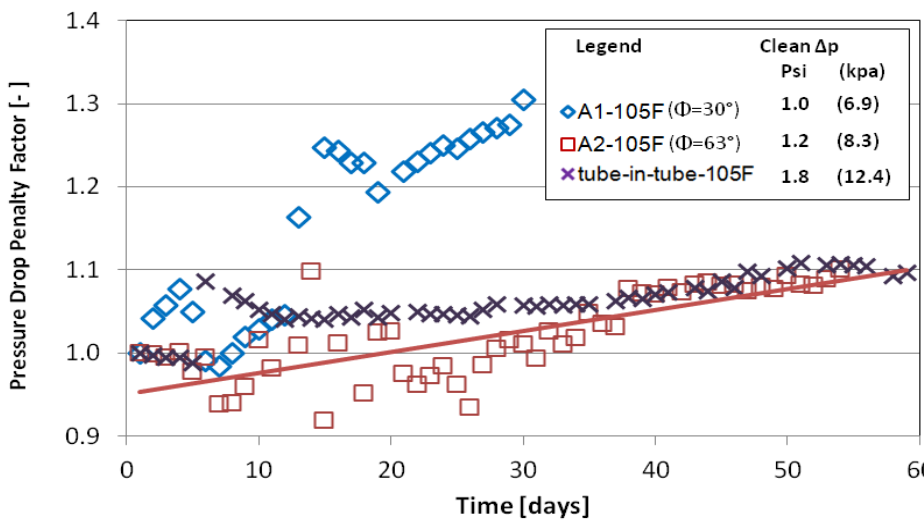

Figure 8: Comparison of measured pressure drop penalty factor between TTHE (tube-in-tube) and BPHEs (A1&A2)

It should be noted that, high fouling potential water (very aggressive water in terms of precipitation) represent severe scaling conditions that should be avoided by proper water treatment of the cooling tower water. Figure 9 shows the effect of water quality on asymptotic fouling resistance. In this figure, both BPHEs and tubular heat exchangers are compared. For A1 plate with soft corrugation angles of 30°, shown as diamond points, the increase of water fouling potential from medium to high, would lead to threefold increase in fouling resistance, that is from 3.3×10^{-4} ft^2-°F-hr/Btu (5.8×10^{-5} m^2-°C/w) to 1.1×10^{-3} ft^2-°F-hr/Btu (1.9×10^{-4} m^2-°C/w) for medium and high fouling potential, respectively. For A2 plate with hard corrugation angle of 63°, an increase of fouling potential augmented the fouling resistance by about 50%. The trends indicate that water fouling potential has a measureable effect on the fouling performance of the heat exchangers. In the current work, the authors experimentally measured the TTHE performance at high fouling potential water while the fouling resistance at medium fouling potential was extrapolated from the data based on the results with A1 and A2 plates. This extrapolation point of the fouling resistance for the TTHE condenser at medium fouling potential is shown as the dashed cross in Figure 9.

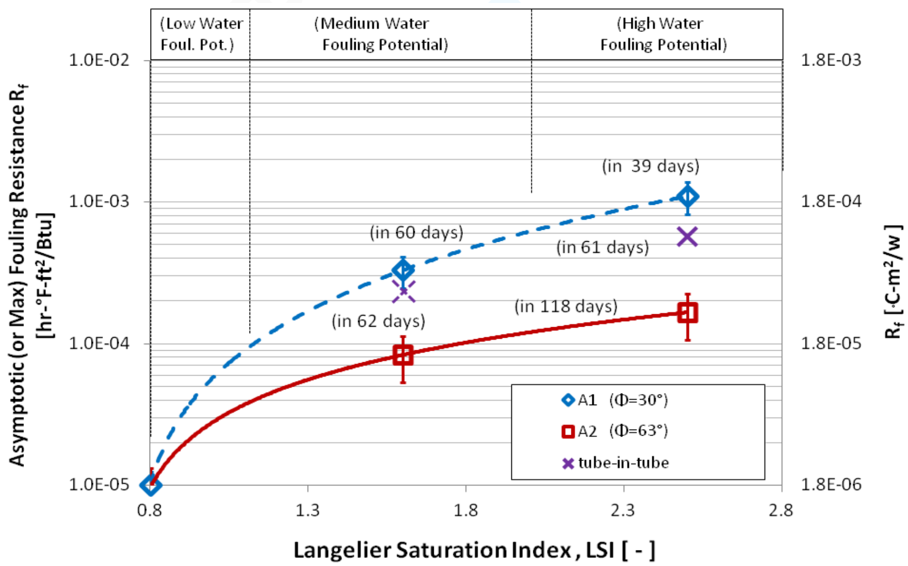

Figure 9: Effect of water quality on asymptotic fouling resistance between TTHE (tube-in-tube) and BPHEs (A1&A2)

5. CONCLUSIONS

Brazed plate heat exchanges (BPHEs) and tube-in-tube heat exchangers (TTHEs) are commonly used in the refrigeration, air conditioning, and food industry as refrigerant-to-water condensers and they often suffer from severe fouling issues. In this work, a smooth TTHE was experimentally investigated and its thermal and hydraulic performance in fouling operating conditions was compared with those for BPHEs with similar heat transfer area and under similar operating conditions. Fouling resistance in BPHEs varies with different corrugation angles and this was due to different local velocity and internal turbulence intensity of the water stream inside the plates. The fouling resistance in TTHE was higher than BPHE with hard corrugation angle but lower than BPHEs with soft corrugation angle. The hydraulic performance of TTHE is more close to BPHEs with hard corrugation angle of 63°. Fouling deposits on the TTHE was sampled and chemical analysis revealed that more than 85% of the fouling was calcium carbonate while the amount of iron, copper and zinc were within 5%. The mineral precipitation mass flux was practically the same for the entire system and the analysis provide an order of magnitude of the mineral precipiation mass flux for the case of high water fouling potential.

NOMENCLATURE

L	length	(in or m)	**Subscripts**	
LSI	Langelier Saturation Index	(-)	EWT	entering water temperature
$\dot{m}$	mass flow rate	(lbm/min or kg/s)	f	fouling or fouled
Δp	pressure difference	(psi or kpa)	LWT	leaving water temperature

PDPF	pressure drop penalty factor	(-)	r	refrigerant
R_f	fouling resistance	(hr-°F-ft^2/Btu or m^2-°C/w)	sat	saturation
ΔT	temperature difference	(°F or °C)	SH	superheat
$\dot{V}$	volume flow rate	(gpm or m^3/s)	w	water
Φ	corrugation angle	(-)		

REFERENCES

AHRI. (2007). *AHRI Standard 450 - Performance Rating of Water-Cooled Refrigerant Condensers, Remote Type*. Arlington, VA, USA: Air-Conditioning, Heating and Refrigeration Institute (AHRI).

Bansal, B., Muller-Steinhagen, H., & Chen, X. D. (2001). Comparison of crystallization fouling in plate and double-pipe heat exchangers. *Heat Transfer Engineering, 22*(Compendex), 13-25.

Chamra, L. M., & Webb, R. L. (1994). Modeling liquid-side particulate fouling in enhanced tubes. *International Journal of Heat and Mass Transfer, 37*(Compendex), 571-579.

Cho, Y. I., Lee, S., & Kim, W. (2003). *Physical water treatment for the mitigation of mineral fouling in cooling-tower water applications.* Paper presented at the Technical and Symposium Papers Presented At the 2003 Winter Meeting of The ASHRAE, January 26, 2003 - January 29, 2003, Chicago, IL, United states.

Cremaschi, L., Spitler, J. D., Lim, E., & Ramesh, A. (2011). Waterside fouling performance in brazed-plate-type condensers for cooling tower applications. *HVAC and R Research, 17*(2), 198-217.

Cremaschi, L., Barve, A., & Wu, X.(2012). Effect of Condensation Temperature and Water Quality on Fouling of Brazed Plate Heat Exchangers. Paper prensented at the ASHRAE winter meeting-Technical Papers, January 21,2012-January 25, Chicago, IL, United States.

Flynn, D. J., & Nalco, C. (2009). The Nalco water handbook. from http://www.knovel.com/knovel2/Toc.jsp?BookID=2799

Grandgeorge, S., Jallut, C., & Thonon, B. (1998). Particulate fouling of corrugated plate heat exchangers. Global kinetic and equilibrium studies. *Chemical Engineering Science, 53*(17), 3050-3071.

Haider, S. I., Webb, R. L., & Meitz, A. K. (1991). *Survey of water quality and its effect on fouling in flooded water chiller evaporators.* Paper presented at the ASHRAE Winter Meeting - Technical Papers, January 19, 1991 - January 23, 1991, New York, NY, USA.

Hasson, D., Sherman, H., & Biton, M. (1978). Prediction of Calcium Carbonate Scaling Rates. *Proceedings 6th Intern. Symposium Fresh Water from the Sea*, *v*(2), 193-199.

Karabelas, A. J., Yiantsios, S. G., Thonon, B., & Grillot, J. M. (1997). Liquid-side fouling of heat exchangers. An integrated R D approach for conventional and novel designs. *Applied Thermal Engineering, 17*(Compendex), 727-737.

Knudsen, J. G., & Story, M. (1978). Effect of Heat Transfer Surface Temperature on the Scaling Behavior of Simulated Cooling Tower Water. *AIChE Symposium Series, 74*(Compendex), 25-30.

Langelier, W. F. (1936). The analytical control of anti-corrosion water treatment. *Journal of American Water Works Association*, 28(10):1500-1521.

Li, W., & Webb, R. L. (2000). Fouling in enhanced tubes using cooling tower water Part II: Combined particulate and precipitation fouling. *International Journal of Heat and Mass Transfer, 43*(Compendex), 3579-3588.

Liu, Z., Shi, M., & Dai, G. (1997). Heat mass transfer model of scaling process. *Huagong Xuebao/Journal of Chemical Industry and Engineering (China), 48*(4), 401-407.

Stasiek, J., Collins, M. W., Ciofalo, M., & Chew, P. E. (1996). Investigation of flow and heat transfer in corrugated passages—I. Experimental results. *International Journal of Heat and Mass Transfer, 39*(1), 149-164.

Taylor, B. N., & Kuyatt, C. E. (1994). *Guidelines for evaluating and expressing the uncertainty of NIST measurements results*. Washington, D. C.: National Institute of Standards and Technology.

Thonon, B., Grandgeorge, S., & Jallut, C. (1999). Effect of geometry and flow conditions on particulate fouling in plate heat exchangers. *Heat Transfer Engineering, 20*(Compendex), 12-24.

Walker, R. (1976). Corrosion Inhibition of Copper by Tolyltriazole. *Corrosion, 32*(Compendex), 339-341.

Xu, Z., Wen, X., Zheng, J., Guo, J., & Huang, X. (2011). Cooling water fouling resistance prediction of plate heat exchanger based on partial least-squares regression. *Huagong Xuebao/CIESC Journal, 62*(6), 1531-1536.

Zan, C., Shi, L., & Ou, H. (2009). Effects of temperature and velocity on fouling by municipal secondary effluent in plate heat exchangers. *Qinghua Daxue Xuebao/Journal of Tsinghua University, 49*(2), 240-243.